2024 46th Annual International Conference of the IEEE Engineering in Medicine and Biology Society (EMBC) | 979-8-3503-7149-9/24/$31.00 ©2024 IEEE | DOI: 10.1109/EMBC53108.2024.10782718

Pruning functional connections in human induced pluripotent stem cell derived neural networks

Shravan Thaploo*, Derrick Lin*, Gregory J. Brewer*, An H. Do†, Zoran Nenadic*
*Department of Biomedical Engineering, University of California Irvine (UCI), Irvine, CA, USA
†Department of Neurology, UCI, Irvine, CA, USA
Email: {znenadic,gjbrewer}@uci.edu, {sthaploo,lindc1,and}@hs.uci.edu

***Abstract*—The failure of human neuronal stem cells to integrate with brain tissue suggests the need to provide functional cues to modify and re-organize the existing naive network. Understanding how human neural networks respond to external stimuli is crucial to realizing this goal. Here, we stimulate a human induced pluripotent stem cell (hIPSC)-derived neural network on a microelectrode array in a Hebbian fashion to explore the resulting network changes. Short exposure to our stimulation protocol resulted in rapid de-correlation of prior functional connections as well as the emergence of a few strong negative connections. Furthermore, stimulation of the network increased median firing rates with observed network reorganization maintained over the course of 15 days.**

***Index Terms*—stem cells, microelectrode arrays, Hebbian learning, neural networks**

I. Introduction

Stroke is one of the leading causes of long-term disability in the United States [1], with no means to reverse the underlying permanent neurological damage. Current stroke rehabilitation therapies rely on residual neural resources to reprise the lost functions. Alternatively, regenerative medicine approaches postulate that stroke-damaged tissue can be replaced using human stem cell-derived neurons. Unfortunately, injecting human induced pluripotent stem cells (hIPSCs) directly into stroke-damaged cortex has not shown considerable improvement in patient neurological outcomes in large-scale multi-center clinical trials [2], [3]. Despite receiving favorable biochemical cues in the brain microenvironment, neural stem cells may lack the behavioral information necessary to functionally integrate with the post-stroke brain and enable functional recovery. This failure to meaningfully connect with surrounding tissue suggests a need to deliver functional cues to encode behavioral information in these renewed neural resources.

Before clinically testing the functional integration of hIPSC-derived neural networks with human brain, the feasibility of this concept must be demonstrated *in vitro*. Fig. 1 conceptually illustrates how this experiment may be designed. We envision a biological neural network being cultured on a standard microelectrode array (MEA), which is capable of supplying input and feedback via electrical stimulation, and recording the network activity to drive the feedback signal. By receiving input and real-time feedback stimulation patterns that are consistent over time, the network may be functionally reorganized to learn the task at hand [4], [5]. The decoder that translates the MEA activity into the feedback signal may be co-adaptively trained in this process or could be fixed according to a pre-defined schema.

Study supported by UCI, the National Science Foundation (Award #2223559), and the National Institute of Health (Award #T32NS082174).

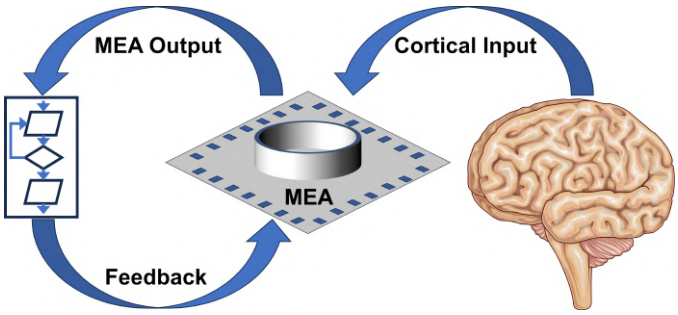

Fig. 1. The interfacing of a biological neural network with the human brain. A network cultured on an MEA receives an input underlying a specific cortical function. Depending on the network's response, a decoder provides feedback to the network. The process runs in a loop until the network learns to reprise the cortical function.

Motivated by this long-term vision, we derived neural progenitor cells and astrocytes from hIPSCs. We then co-cultured these cells on an MEA and maintained the network over several months. Once the network matured and became electrically active, we delivered consistently paired electrical stimulation patterns at two different MEA locations, thus mimicking the effect of cortical input and feedback. Unlike Fig. 1, our stimulation paradigm was neither designed to encode any specific function nor executed in a closed loop. Still, since the near co-incident activation of two groups of neurons may induce Hebbian plasticity, we sought to investigate its effect in a mature co-culture. To this end, we characterized the network's spontaneous behavior and functional properties before and after subjecting it to this stimulation paradigm.

II. Methods

A. Overview

A biological neural network consisting of hIPSC-derived neurons and astrocytes was cultured and matured on a glass microelectrode arrays (MEA). By producing extracellular matrix and trophic factors, astrocytes could enhance culture viability [6]. Once the network became electrically active, as ascertained by the presence of spontaneous action potentials

(APs), we characterized its behavior by recording its spontaneous activity. We then stimulated the network by delivering electrical pulses in a precise temporal order at two pre-defined locations. Upon stimulation, we quantified and characterized the changes in network's spontaneous behavior.

B. Neural Network Culturing and Maturation

The network was cultured and matured on a glass MEA (60MEA200/30iR-ITO-gr, Multichannel Systems, Reutlingen, Germany). Prior to culturing, we treated the MEA surface as follows. First, we O_2-plasma treated the MEA with silicon nitride passivation at 100 W and 0.2 mbar for 1.5 minutes. We subsequently coated the glass surface with a poly-D-lysine solution (PDL) (100 μg/mL, Sigma, Burlington, MA) in a sterile fashion. We then aspirated the PDL solution, gently washed the MEA surface with sterile deionized (DI) water (18 MΩ), and air-dried the MEA. Finally, we applied human recombinant vitronectin (Gibco, Carlsbad, CA) at a 0.5 μg/cm$_2$ concentration to the modified surface for one hour. We deposited hIPSC-derived neural progenitor cells and astrocytes onto the MEA at a total concentration of 5.5×10^4 cells/cm^2 ($\sim$1:1 ratio), similar to literature reports [7], [8]. This co-culture was maintained with a combination of BrainPhys medium supplemented with N2 [StemCell Technologies, Vancouver, CA], SM1 [B27 equivalent] and ascorbic acid within a 37°C, 99% humidity, 5% CO_2 incubator to facilitate maturation. We changed $\sim$50% of medium every 2-3 days.

C. Electrophysiological Recording and Stimulation System

We interfaced the MEA with a custom-made signal acquisition system (see Fig. 2). Specifically, we designed and fabricated a printed circuit board (PCB) that connected the MEA to a low-cost electrophysiology system. To accommodate recording from up to 64 channels while enabling electrical stimulation, we interfaced our PCB with four stimulation/recording chips (RHS 2116, Intan Technologies, Santa Monica, CA). This stimulation/recording array is capable of recording broadband electrophysiological signals at a 16-bit resolution and sampling rate of up to 30 kHz/channel. It can also deliver biphasic constant-current stimulation pulses ranging from 10 nA to 2.5 mA. The recording and stimulation processess were managed by the RHS stimulation/recording controller (Intan Technologies, Santa Monica, CA).

D. Recording and Stimulation Procedures

Prior to each recording and/or stimulation experiment, we changed $\sim$50% of the co-culture medium under a sterile laminar flow hood. We performed all recording and stimulation experiments at 37°C in a heat-controlled incubator (Fig. 2). We used the Intan controller's impedance measurements and visual inspection to identify and disconnect channels with poor signal quality. Broadband electrophysiological signals were acquired at a rate of 30 kHz, with a 60-Hz notch filter enabled and Intan amplifier bandwidth set to 1 - 15,000 Hz. For stimulation, we used a biphasic square pulse (5 μA, phase width 200 μs). A single stimulation sequence consisted of 40 pulses with the pulse train frequency of 1 Hz.

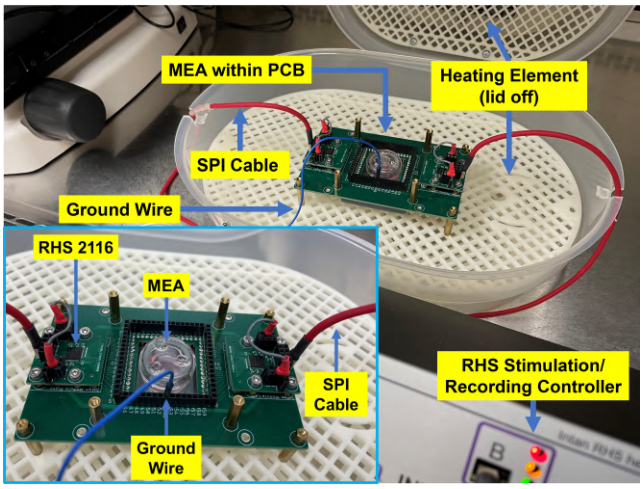

Fig. 2. Recording setup showing custom printed circuit board (PCB) and enclosed MEA. Two serial peripheral interface (SPI) cables connect the RHS 2116 chips to the RHS stimulation/recording controller. Two chips are visible from this perspective, with the other two mounted on the bottom side. The entire assembly is placed within a 37°C heating element under sterile laminar air flow. *Inset:* Close-up view of PCB with the MEA covered by a glass lid. Ground wire is used to mitigate ambient noise.

E. Identifying Stimulation Targets

Before conducting the paired stimulation experiment, we identified target channels for stimulation. To this end, we recorded the network's spontaneous activity over a 40-s period. We used an unsupervised method based on the continuous wavelet transform to detected APs and estimate their arrival times [9]. Finally, we selected the channel with the highest activity as the input channel (I) (see Fig. 3.)

We selected the feedback channel (F) based on two criteria. First, to minimize potential coupling through volume conduction, we constrained the feedback channel to be $\geq$800 μm away from the input channel. Secondly, we searched for a channel that was not "synaptically coupled" to the input channel. To this end, we delivered the 40-s stimulation sequence to the input channel while recording the response of all other channels. We then analyzed these data to determine whether the firing patterns of channels changed in response to the stimulation. Specifically, for each channel, we compared the number of APs in a 250-ms window before and after each stimulation pulse and used a two-tailed sign test to ascertain statistical significance. Channels that were not significantly affected by stimulating the input channel and were sufficiently far from it were deemed feedback channel candidates, among which one was ultimately selected (Fig. 3).

F. Paired Stimulation Protocol

All experiments were performed at 85 DIV with intent to induce short-term network plasticity. We first collected $\sim$40 s of spontaneous activity data to characterize the behavior and functional connectivity of a "naive" network. We will refer to these data as the *baseline 1* condition. Subsequently, we delivered paired stimulation to the input and feedback channels using the standard pulse sequence (see Section II-D).

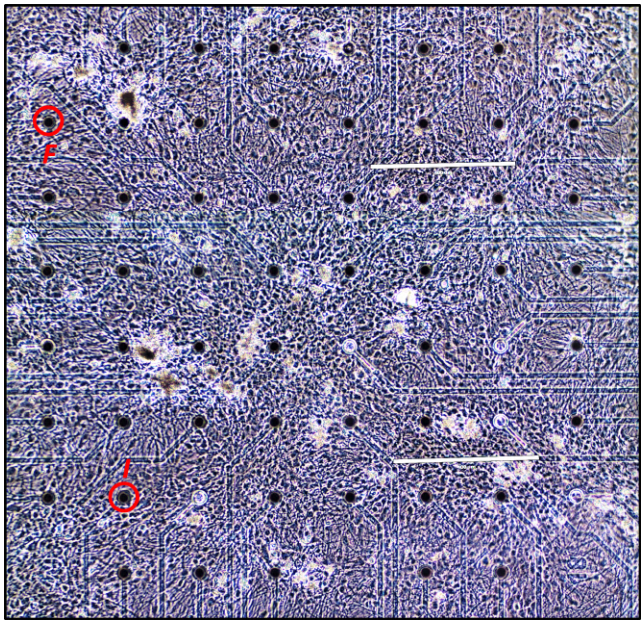

Fig. 3. Composite phase-contrast microscopy (10×) image of the culture at 85 days-in-vitro (DIV) showing 100% confluence. Encircled electrodes mark the locations of the input (I) and feedback (F) channels. Electrodes visible as white circles exhibit signs of degradation. The scale bars are 400 μm.

To mimic a low-latency feedback, we imposed a 25-ms delay between the input and feedback stimulation sequences. We delivered 15 stimulation sequences (600 pulses) at both the input and feedback channels, with a 1-min break between the successive sequences. Immediately upon completing this process, we recorded the spontaneous activity again. We will refer to this condition as *baseline 2*. We observed gradual changes in medium color during stimulation, suggesting a change in pH conditions. We hypothesize that this may have been caused by a lack of CO_2 control under the laminar flow hood. To control for these factors, we performed a 50% medium change and immediately repeated the measurement of network spontaneous activity. We will refer to this condition as *baseline 3*.

G. Network Analysis

Stored MEA signals were analyzed in MATLAB (MathWorks, Natick MA) with custom scripts. The APs were detected using the unsupervised wavelet method, which makes few prior assumptions regarding the shape of APs, and as such provides less biased detection results [9], [10]. We subsequently converted the AP arrival times into firing rates (FRs) on a per channel basis by binning the AP counts into one-second-long, non-overlapping intervals. The non-overlapping intervals minimized the temporal correlations in the FRs, thereby providing more accurate statistical tests (see below). Channels exhibiting low AP rates, defined as less than four APs in a 40-s interval (<0.1 AP/s), were assigned a zero FR. This excluded channels for which defining FR made no sense due to their sparse response. It also precluded spurious correlations between channels (see below). We then cross-correlated FRs (zero lag) across the channels. The correlation coefficients that were not deemed statistically significant ($\alpha = 0.01$) were set to zero. Finally, we characterized and compared these functional networks across the three experimental conditions.

TABLE I
MAXIMUM AND MEDIAN FIRING RATES (APS/S) ACROSS THE THREE CONDITIONS, AS WELL AS THE NUMBER OF CHANNELS WITH NO APS AND LOW AP RATE (<0.1 HZ).

Condition	max	median	chan. with no APs	chan. low AP rate
baseline 1	135	8	3	2
baseline 2	139	1	1	8
baseline 3	133	14	2	2

TABLE II
THE TOTAL NUMBER OF UNIQUE FUNCTIONAL CONNECTIONS, THE NUMBER OF NEGATIVE CONNECTIONS, AND THE TOTAL NUMBER OF CONNECTIONS EMANATING FROM THE INPUT AND FEEDBACK CHANNELS.

Condition	total	negative	channel #2 (I)	channel #35 (F)
baseline 1	540	0	34	21
baseline 2	117	1	14	2
baseline 3	175	2	22	7

III. RESULTS

Fig. 4 shows the spontaneous network activity prior to paired stimulation (*baseline 1* condition). Individual APs were detected as described above. Of the 48 channels that had useful signals, three channels did not have any detectable APs. Two channels had APs but exhibited low AP rates (<0.1 AP/s).

Fig. 5 shows the firing rates across the three conditions. Immediately upon paired stimulation (*baseline 2*), the network's activity became more suppressed. For example, while the most active channel (channel #2) retained the high FR, reaching values as high as 139 APs/s, its average FR (across the 40-s interval) decreased from 85 to 45 APs/s. Similarly, the median FR (across all channels and time windows) decreased from eight to one AP/s (see Table I). At the same time, the number of channels with low AP rate increased from two to eight. Upon medium change (*baseline 3*), the network activity was restored and generally exceed that of the *baseline 1* condition. Specifically, the median FR increased to 14 APs/s, while the number of channels with low AP rates decreased back to two.

Fig. 6 shows the correlations of FRs across all channel pairs. In the *baseline 1* condition, there were 540 functional connections (statistically significant correlations), suggesting an overly connected functional network (see Table II). Upon paired stimulation *baseline 2*, the number of connections decreased to 117, as evidenced by the disappearance of large high-correlation blocks (see Fig. 6). While some of these connections were restored upon medium change (*baseline 3*), the network generally remained sparsely connected. The functional connections emanating from the input and feedback channels showed a similar trend (see Table II. Finally, both post-stimulation conditions exhibited a small number of negatively correlated channels, suggesting the emergence of inhibition. Note that inhibitory connections were not observed in the *baseline 1* condition.

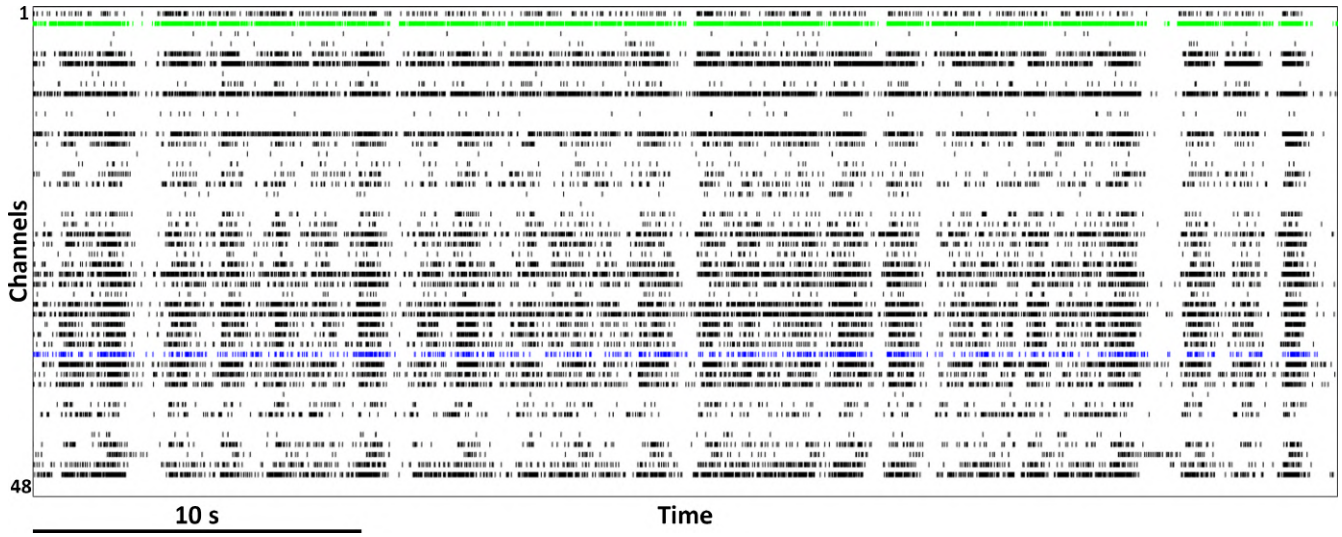

Fig. 4. Raster plots showing the occurrence of individual APs across 48 MEA channels during the *baseline 1* condition. Raster plots marked in green and blue highlight the input and feedback channels, respectively. Equivalent plots for the *baseline 2* and *baseline 3* conditions are omitted due to space constraints.

IV. Discussion

We present a preliminary exploration of the effect of repeated paired electrical stimulation on hIPSC-derived neural network properties. By delivering paired stimulation to our co-culture at two different channels, we sought to characterize its spontaneous functional network properties and behavior. After delivering stimulation, we discovered changes in the average firing rate, and the number and type of functional connections across all channels within the network. The immediate effect of stimulation is suppression of APs (*baseline 2*), with suppression reversed after a medium change (*baseline 3*). As stimulation was performed without CO_2 control, the reduced firing rate observed in the *baseline 2* condition may be attributed to media pH changes. The increase in median firing rate across all channels seen in *baseline 3* indicates changes in channel correlations are not driven by firing rate. Interestingly, the total number of functional connections after stimulation is significantly reduced, with this reduction mostly conserved after medium change. Together, these results suggest that our stimulation protocol induced a rapid de-correlation of the network. The loss of correlation across multiple channels, with the emergence of strongly negative functional connections suggests a fundamental reorganization of the network following our stimulation protocol.

Our study is limited by a small sample size and the changes seen in our network could be transient. To investigate whether the rapid de-correlation of the network after stimulation is conserved, we repeated our stimulation protocol after 15 days (DIV 100). Our preliminary results indicate that the pruning of functional connections and the existence of negative connections are preserved. However further experiments are required to ascertain long-term stability of these changes.

Interfacing a hIPSC-derived neural network on a MEA with cortical inputs from a human brain could provide an engineered approach to encode behavioral information into these cells, ultimately forming a neuro-restorative approach to stroke. However, realizing this possibility requires a deeper understanding of how biological networks respond to external stimulation. This study represents an initial step towards achieving this goal.

References

[1] C. for Disease Control, P. (CDC, *et al.*, "Prevalence of stroke–united states, 2006-2010," *MMWR. Morbidity and mortality weekly report*, vol. 61, no. 20, pp. 379–382, 2012.

[2] D. Kalladka, J. Sinden, K. Pollock, C. Haig, J. McLean, W. Smith, A. McConnachie, C. Santosh, P. M. Bath, L. Dunn, *et al.*, "Human neural stem cells in patients with chronic ischaemic stroke (pisces): a phase 1, first-in-man study," *The Lancet*, vol. 388, no. 10046, pp. 787–796, 2016.

[3] K. W. Muir, D. Bulters, M. Willmot, N. Sprigg, A. Dixit, N. Ward, P. Tyrrell, A. Majid, L. Dunn, P. Bath, *et al.*, "Intracerebral implantation of human neural stem cells and motor recovery after stroke: multicentre prospective single-arm study (pisces-2)," *Journal of Neurology, Neurosurgery & Psychiatry*, 2020.

[4] B. J. Kagan, A. C. Kitchen, N. T. Tran, F. Habibollahi, M. Khajehnejad, B. J. Parker, A. Bhat, B. Rollo, A. Razi, and K. J. Friston, "In vitro neurons learn and exhibit sentience when embodied in a simulated game-world," *Neuron*, vol. 110, no. 23, pp. 3952–3969, 2022.

[5] T. B. DeMarse and K. P. Dockendorf, "Adaptive flight control with living neuronal networks on microelectrode arrays," in *Proceedings. 2005 IEEE International Joint Conference on Neural Networks, 2005.*, vol. 3, pp. 1548–1551, IEEE, 2005.

[6] S. Wiese, M. Karus, and A. Faissner, "Astrocytes as a source for extracellular matrix molecules and cytokines," *Frontiers in pharmacology*, vol. 3, p. 120, 2012.

[7] StemCell Technologies, Vancouver, Canada, *BrainPhys Product Information Sheet*, 2024.

[8] D. A. Wagenaar, J. Pine, and S. M. Potter, "Effective parameters for stimulation of dissociated cultures using multi-electrode arrays," *Journal of neuroscience methods*, vol. 138, no. 1-2, pp. 27–37, 2004.

[9] Z. Nenadic and J. W. Burdick, "Spike detection using the continuous wavelet transform," *IEEE Transactions on Biomedical Engineering*, vol. 52, no. 1, pp. 74–87, 2005.

[10] R. Benitez and Z. Nenadic, "Robust unsupervised detection of action potentials with probabilistic models," *IEEE Transactions on Biomedical Engineering*, vol. 55, no. 4, pp. 1344–1354, 2008.

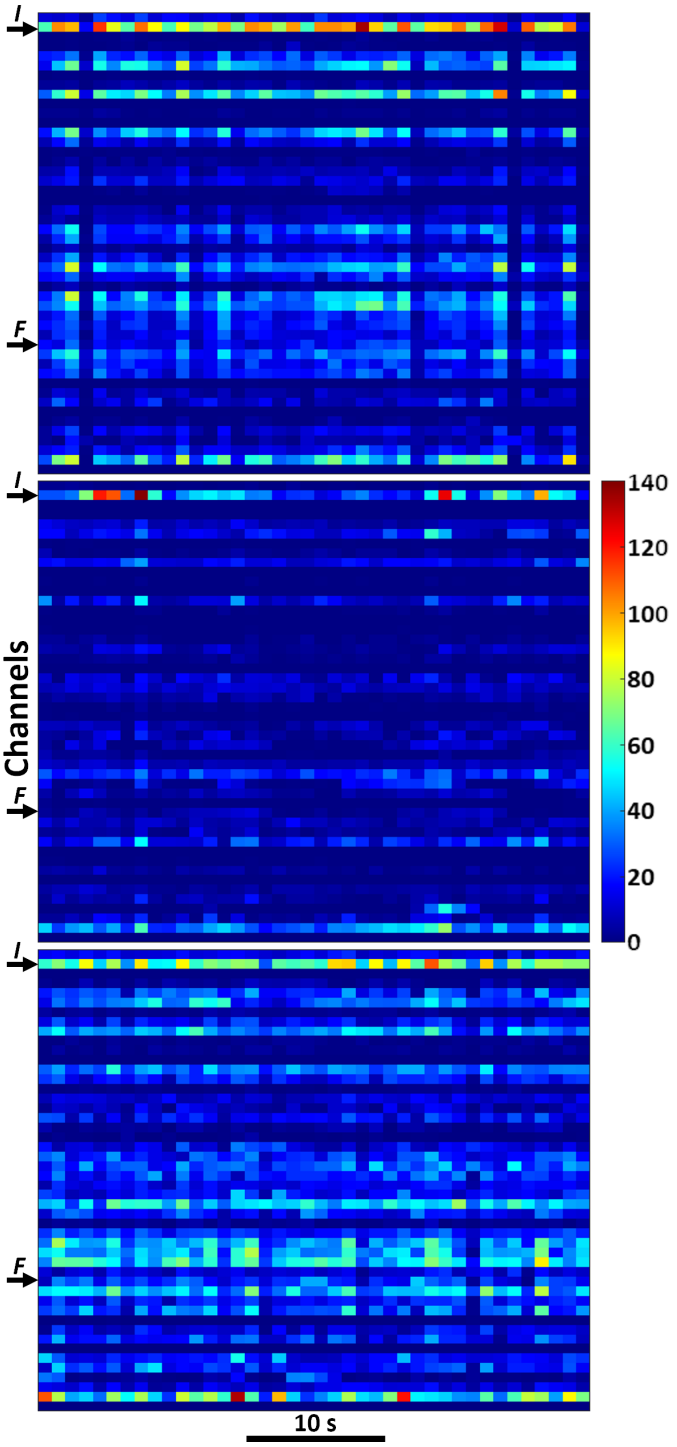

Fig. 5. (Top) Firing rates (AP/s) corresponding to the *baseline 1* condition (cf. Fig. 4). Arrows indicate the input (I) and feedback (F) channels used to deliver paired stimulation. Note that paired stimulation was delivered after the *baseline 1* condition, but before the *baseline 2* and *baseline 3* conditions. (Middle) The equivalent data for the *baseline 2* condition. (Bottom) Firing rates corresponding to the *baseline 3* condition.

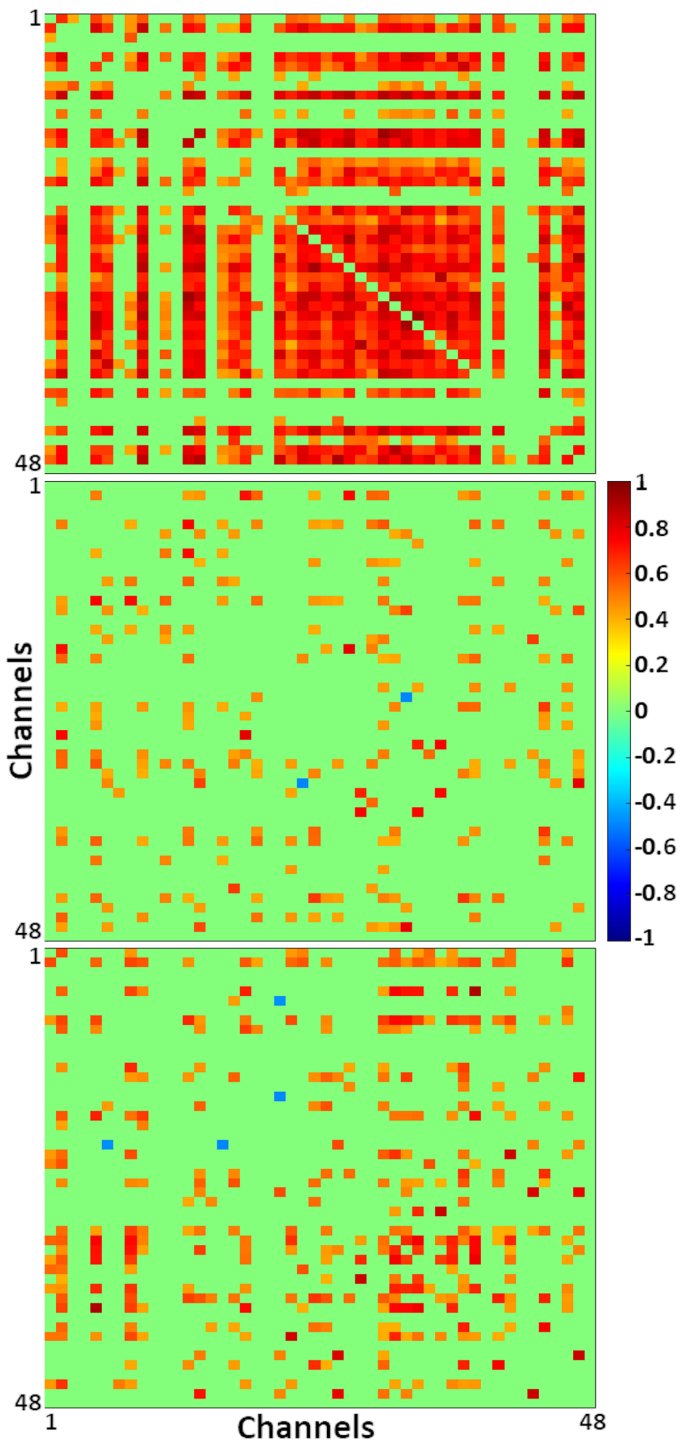

Fig. 6. (Top) Correlation coefficient matrix corresponding to the FRs of *baseline 1* condition (cf. Fig. 5). The coefficients that were not statistically significant were set to zero (Middle) The equivalent data for the *baseline 2* condition. (Bottom) Correlation coefficients of the *baseline 3* condition.